Supplement of Hydrol. Earth Syst. Sci., 29, 4739–4759, 2025
https://doi.org/10.5194/hess-29-4739-2025-supplement

Hydrology and Earth System Sciences
Open Access

Supplement of

Skilful seasonal streamflow forecasting using a fully coupled global climate model

Gabriel Fernando Narváez-Campo and Constantin Ardilouze

Correspondence to: Gabriel Fernando Narváez-Campo (gabriel.narvaez-campo@umr-cnrm.fr)

This document provides supplementary material to illustrate the analyses further and add additional details to the discussion of the current research article.

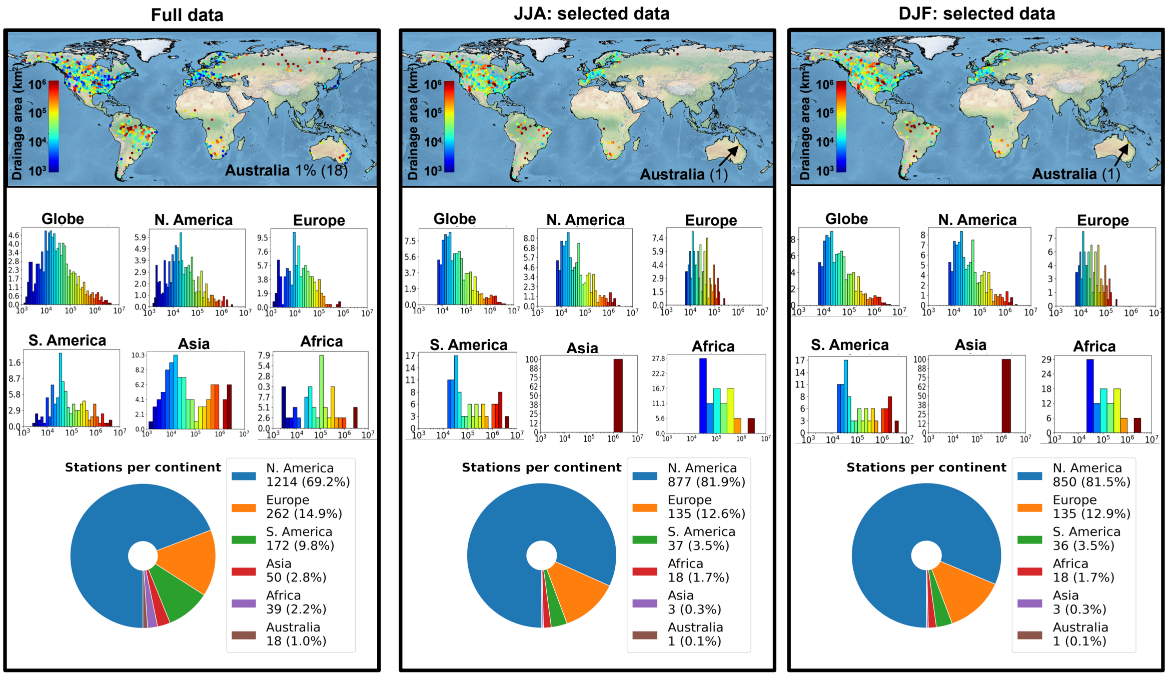

Figure S1. Full global streamflow database and selected database (per season). From the full global database of 1755 streamflow stations, only those with a drainage area higher than 6×10^3 km^2 and less than 25% of missing data (in the corresponding season) are selected. Then, we have 1071 and 1043 stations for JJA and DJF, respectively.

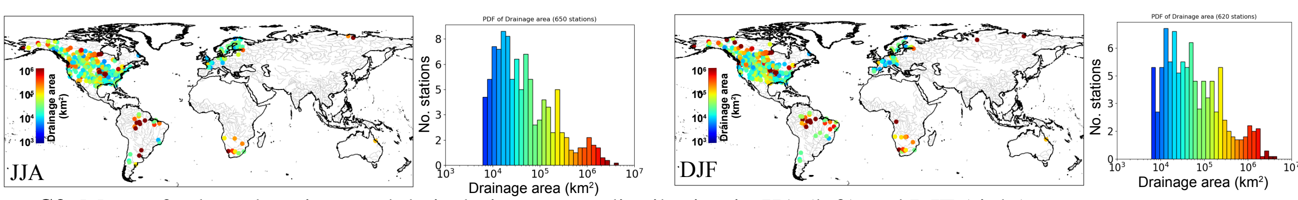

Figure S2. Maps of selected stations and their drainage area distribution in JJA (left) and DJF (right).

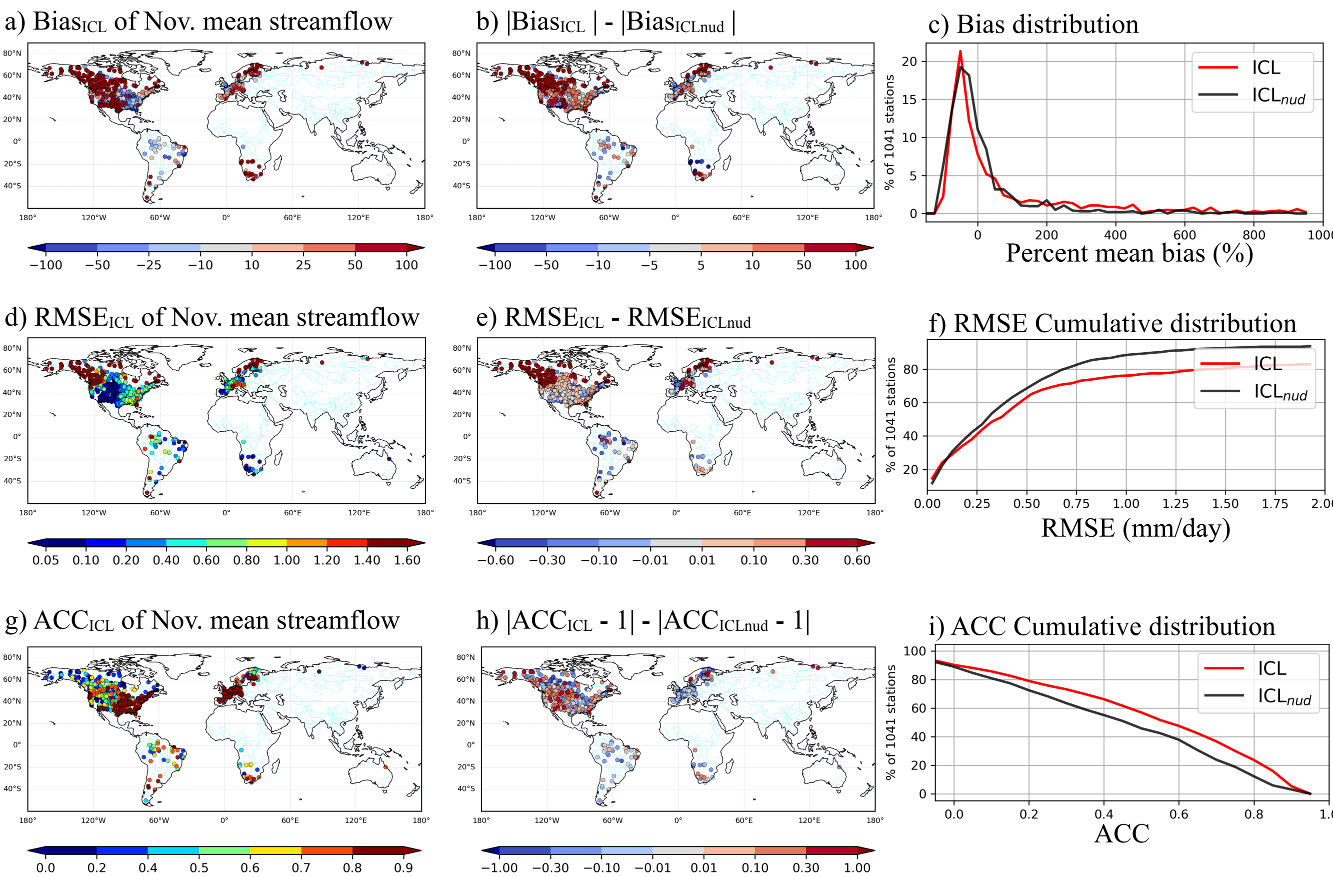

Figure S3. Comparison between November streamflow mean of initialisation run against the observed one over 1993-2017. Left column: ICL bias (a), root mean square error (mm/d) (d), anomaly correlation (g). Middle column: difference with the ICL_{nud} enhanced land initialisation bias (b), root mean square error (mm/d) (e), anomaly correlation (h). Right column: distribution of bias for each experiment (c), accumulated distributions of the root mean square (f), and anomaly correlation (i).

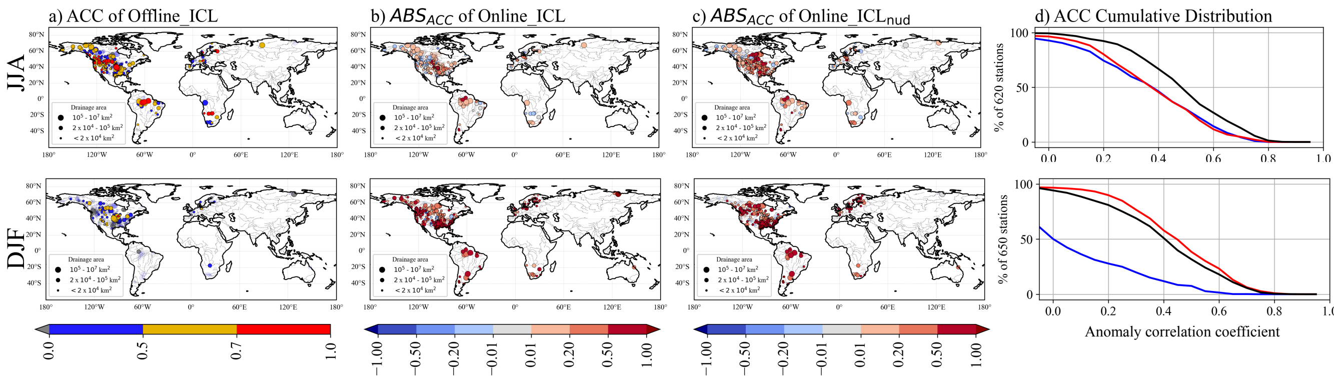

Figure S4. ACCs of bias-corrected streamflow hindcasts computed against observation in JJA (first row) and DJF (second row). ACCs of Offline_ICL benchmark (a) and the corresponding absolute skill score ABS of ACC for the online coupled configurations with conventional initialisation (b) and improved initialisation (c). Cumulative distribution of the anomaly correlation coefficient (d). This figure presents the stations where at least one hindcast provides ACC ≥ 0.6 and no negative lower confidence interval with a 95% of confidence level.

Figure S5 shows the cumulative frequency distributions of ACC for each of the four months forecasted. From the figure, we can remark on the following points.

- As expected, the performance decreases with lead time in all the forecast system configurations.
- In boreal summer JJA, the hindcast with improved land initialisation Online_ICL$_{nud}$ outperforms Offline_ICL benchmark at all lead time months. Conversely, Online_ICL is better than Offline_ICL for lead times over one month, as indicated by the slightly higher number of stations with positive but low correlations (about ACC<0.3).
- In boreal winter DJF, Online_ICL and Online_ICL$_{nud}$ performance is similar but always better than the Offline_ICL. Online_ICL is slightly better than Online_ICL$_{nud}$ in January (for 0.2<ACC<0.6) and February predictions (0.1<ACC<0.3).

The remarks are consistent with the conclusions derived from the 3-month discharge mean presented in the manuscript.

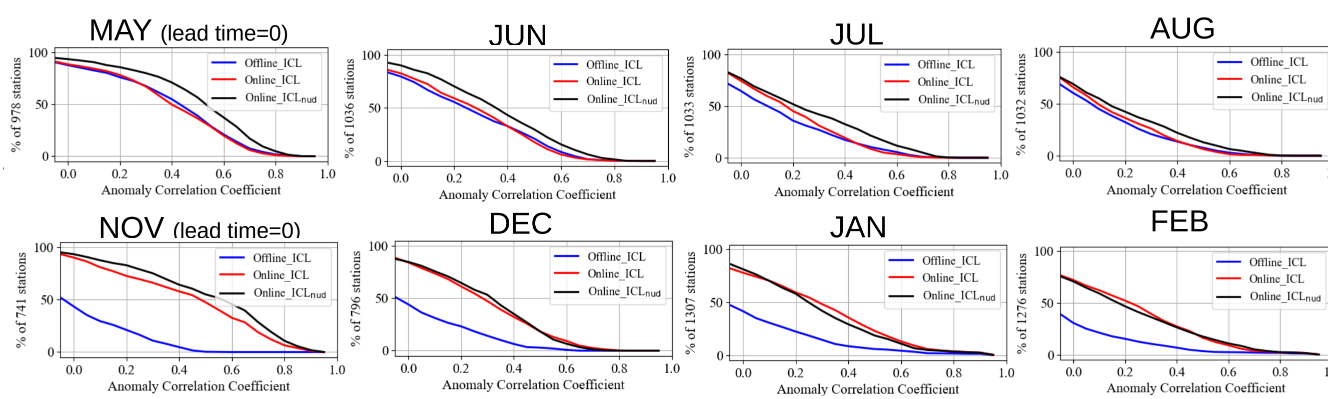

Figure S5. Global performance of forecasting systems at different lead times for summer JJA and winter DJF boreal seasons. The anomaly correlation coefficient for 1993-2017.